nebulin are interdependent. Therefore, the precision and tissue specificity of the sarcomeric assembly program in vertebrates appear to necessitate coordinated splicing decisions in the titin and nebulin precursor mRNAs.

REFERENCES AND NOTES

1. K. Maruyama, *Biophys. Chem.* **50**, 73 (1994); J. Trinick, *Trends Biochem. Sci.* **19**, 405 (1994).
2. K. Wang, J. McClure, A. Tu, *Proc. Natl. Acad. Sci. U.S.A.* **76**, 3698 (1979).
3. K. Maruyama *et al.*, *J. Biochem. (Tokyo)* **82**, 317 (1977).
4. R. Nave, D. O. Fürst, K. Weber, *J. Cell Biol.* **109**, 2177 (1989); J. Suzuki, S. Kimura, K. Maruyama, *J. Biochem. (Tokyo)* **116**, 406 (1994).
5. In the microscope, striated muscle appears as a periodical array of darker and brighter stripes. The dark segment contains the thick filament (myosin) and is referred to as the A band, the bright segment contains the thin filament (actin) and is called the I band. In the center of A and the I bands, dense structures ~100 nm wide are present, referred to as M lines and Z discs, respectively. A single titin molecule spans the distance from the Z disc to the M line [D. O. Fürst, M. Osborn, R. Nave, K. Weber, *J. Cell Biol.* **106**, 1563 (1988)].
6. S. Labeit, M. Gautel, A. Lakey, J. Trinick, *EMBO J.* **11**, 1711 (1992).
7. A. Soteriou, M. Gamage, J. Trinick, *J. Cell Sci.* **104**, 119 (1993).
8. Y. Itoh *et al.*, *J. Biochem. (Tokyo)* **104**, 504 (1988).
9. A. Magid and D. J. Law, *Science* **230**, 1280 (1985).
10. R. Horowits, E. S. Kempner, M. E. Bisher, R. J. Podolsky, *Nature* **323**, 160 (1986); T. Funatsu, H. Higuchi, S. Ishiwata, *J. Cell Biol.* **110**, 53 (1990); G. Salviati, R. Betto, S. Ceoldo, S. Pierobon-Bormioli, *Am. J. Physiol.* **259**, C144 (1990).
11. T. Funatsu *et al.*, *J. Cell Biol.* **120**, 711 (1993).
12. A monoclonal antibody raised to an expressed titin kinase domain fragment stains sarcomeres in the periphery of the M line region (D. O. Fürst, unpublished material).
13. M. Gautel, K. Leonard, S. Labeit, *EMBO J.* **12**, 3827 (1993).
14. C. Hill and K. Weber, *J. Cell Biol.* **102**, 1099 (1986).
15. K. Wang, R. McCarter, J. Wright, J. Beverly, R. Ramirez-Mitchell, *Proc. Natl. Acad. Sci. U.S.A.* **88**, 7101 (1991); R. Horowits, *Biophys. J.* **61**, 392 (1993); H. L. Granzier and T. C. Irving, *ibid.* **68**, 1027 (1995).
16. B. Kolmerer and S. Labeit, unpublished material.
17. The inclusion of the 22.5 kb of sequences between I15 and I20 predicts that soleus titin is encoded by a 101-kb mRNA, encompasses 33,000 residues, and has a molecular mass of 3700 kD.
18. R. Craig, *J. Mol. Biol.* **109**, 69 (1977); ——— and G. Offer, *Proc. R. Soc. London Ser. B.* **192**, 451 (1976); M. Sjöström and J. Squire, *J. Mol. Biol.* **109**, 49 (1977).
19. A 1.8-kb cDNA probe of C zone titin strongly cross-hybridizes to a variety of vertebrate DNAs, from humans to turtles, and detects conserved fragment lengths in most mammalian species (C. Witt and H. Jockusch, unpublished material).
20. The titin exon Mex5 encoding the domain is7 is expressed in all striated muscles; the exon Mex5 is differentially expressed in correlation with M line structure (B. Kolmerer, unpublished results).
21. H. M. Holden, M. Ito, D. J. Hartshorne, I. Rayment, *J. Mol. Biol.* **227**, 840 (1992); M. Pfuhl and A. Pastore, *Structures* **3**, 391 (1995).
22. A. Soteriou, A. Clarke, S. Martin, J. Trinick, *Proc. R. Soc. London Ser. B.* **254**, 83 (1993); H. Erickson, *Proc. Natl. Acad. Sci. U.S.A.* **91**, 10114 (1994).
23. A. S. Politou, D. J. Thomas, A. Pastore, *Biophys. J.*, in press.
24. K. Wang, R. McCarter, J. Wright, J. Beverly, R. Ramirez-Mitchell, *ibid.* **64**, 1161 (1993).
25. K. Trombitas and G. H. Pollack, *J. Muscle Res. Cell Motil.* **14**, 416 (1993).
26. S. Labeit and B. Kolmerer, *J. Mol. Biol.* **248**, 308 (1995).
27. J. A. Aarli, K. Stefansson, L. S. G. Marton, R. L. Wollmann, *Clin. Exp. Immunol.* **82**, 284 (1990).
28. For the main immunogenic region (MIR) of titin, patients' sera (*27*) were used to screen a human cardiac gt11 library, and the isolated phage inserts were expressed in *Escherichia coli*. Protein immunoblots and enzyme-linked immunosorbent assays with recombinant titin antigens assigned the MIR to I45 and I46 [M. Gautel *et al.*, *Neurology* **43**, 1581 (1993)]. T12 (*5*) monoclonal antibody was used to screen a gt11 library. Positive phages were sequenced from both ends and identified a region of overlap within I2 and I3.
29. Single-letter abreviations for the amino acids are as follows: A, Ala; , C, Cys; D, Asp; E, Glu; F, Phe; G, Gly; H, His; I, Ile; K, Lys; L, Leu; M, Met; N, Asn; P, Pro; Q, Gln; R, Arg; S, Ser; T, Thr; V, Val; W, Trp; Y, Tyr; and X, any residue.
30. The cDNA sequences were obtained from commercially available cDNA libraries: human cardiac, Stratagene catalog number 936208; human skeletal, Clontech HL1124.
31. K. Maruyama *et al.*, *Biochem. Biophys. Res. Commun.* **194**, 1288 (1993).
32. For reverse transcriptase–polymerase chain reaction (RT-PCR), human RNAs were prepared essentially as described [R. J. MacDonald, G. H. Swift, A. E. Przybyla, J. M. Chirgwin, *Methods Enzymol.* **152**, 219 (1987)]. Reverse transcription was performed with Moloney murine leukemia virus RT from BRL as specified by the supplier. RT reactions were analyzed by PCR with the use of combinations of primer pairs derived from the cardiac and skeletal sequences [R. K. Saiki *et al.*, *Science* **230**, 1350 (1985)].
33. The 22.5 kb of skeletal I band titin included between I15 and I20 were amplified by PCR as a set of 18 subfragments. Total RNA was blotted on nylon membranes, cross-linked, and hybridized as described, except that temperatures were lowered to 55°C to account for the species difference of the probe and RNA [G. M. Church and W. Gilbert, *Proc. Natl. Acad. Sci. U.S.A.* **81**, 1991 (1984)]. Probes P1 through P18 were labeled randomly essentially as described [A. P. Feinberg and B. Vogelstein, *Anal. Biochem.* **13**, 6 (1983)].

34. We thank J. Trinick for his contributions in the initial stages of this project, M. Saraste, A. Pastore, B. Bullard, K. Leonard, and M. Gautel for their continuous support and encouragement, D. O. Fürst and K. Weber and C. Witt and H. Jockusch for communicating unpublished results, and the Chirugische Kinik Heidelberg for human muscle tissues from organ transplant donors. We gratefully acknowledge the financial support of the Deutsche Forschungsgemeinschaft, the European Community, the Human Frontier Science programme, and the Frauenklinik Mannheim. The 82-kb cardiac titin cDNA and the 22-kb I band titin cDNA included in soleus skeletal muscle have been submitted to the European Molecular Biology Laboratory (EMBL) data library (accession numbers AC X90568 and X90569, respectively). The coordinates of the P1 through P18 subfragments are included in the annotations to accession number X90569; the DNA is available from us. Additional information on the titin sequence and available cDNA and genomic probes can be obtained from the World Wide Web from http://www.aaas.org/science/science.html; see "Beyond the Printed Page."

25 May 1995; accepted 18 August 1995

Requirement for Generation of H_2O_2 for Platelet-Derived Growth Factor Signal Transduction

Maitrayee Sundaresan, Zu-Xi Yu, Victor J. Ferrans, Kaikobad Irani, Toren Finkel*

Stimulation of rat vascular smooth muscle cells (VSMCs) by platelet-derived growth factor (PDGF) transiently increased the intracellular concentration of hydrogen peroxide (H_2O_2). This increase could be blunted by increasing the intracellular concentration of the scavenging enzyme catalase or by the chemical antioxidant *N*-acetylcysteine. The response of VSMCs to PDGF, which includes tyrosine phosphorylation, mitogen-activated protein kinase stimulation, DNA synthesis, and chemotaxis, was inhibited when the growth factor–stimulated rise in H_2O_2 concentration was blocked. These results suggest that H_2O_2 may act as a signal-transducing molecule, and they suggest a potential mechanism for the cardioprotective effects of antioxidants.

Evidence from both plant and animal cells suggests that H_2O_2 may act as an intracellular second messenger. Hydrogen peroxide may regulate the defense of plants against viral pathogens by serving as a small diffusible molecule to orchestrate the hypersensitive response (*1*). Salicylic acid binds to and inactivates tobacco catalase, leading to a rise in H_2O_2 concentration ($[H_2O_2]$) and the activation of gene expression (*2*). In mammalian cells, H_2O_2 has been implicated as an indirect activator of the transcription factor nuclear factor kappa B (NF-κB) (*3*). Because NF-κB modulates the expression of a variety of immune and inflammatory molecules, it would appear that a role for H_2O_2 in host defense mechanisms has been conserved from plants to animals. Similarly, H_2O_2 may function in triggering apoptosis in both plant and animal cells (*1*, *4*).

Stimulation of various mammalian cell types with either cytokines, phorbol esters, or growth factors increases the secretion of

M. Sundaresan, K. Irani, T. Finkel, Cardiology Branch, National Heart, Lung, and Blood Institute (NHLBI), National Institutes of Health (NIH), Bethesda, MD 20892–1650, USA.
Z.-X. Yu and V. J. Ferrans, Pathology Section, NHLBI, NIH, Bethesda, MD 20892–1518, USA.
*To whom correspondence should be addressed

H_2O_2 into the extracellular space (*5*, *6*). We investigated the possibility that a parallel between nitric oxide (NO) and H_2O_2 might exist. High concentrations of these diffusible reactive oxygen intermediates play a role in host defense; however, at low concentrations, NO modulates signal transduction of endothelial and neuronal cells. To evaluate whether H_2O_2 could have a similar function in signal transduction, we studied VSMCs for which low concentrations of exogenous H_2O_2 are mitogenic (*7*).

PDGF stimulation of primary rat VSMCs revealed an increase in intracellular [H_2O_2] as measured by the oxidation of the peroxide-sensitive fluorophore 2′,7′-dichlorofluorescin (DCF). Microfluorometric study with confocal microscopy showed that, compared with quiescent cells, stimulation with the PDGF-AB isoform (5 ng/ml) rapidly increased DCF fluorescence by 50- to 100-fold. The PDGF-stimulated increase in [H_2O_2] is transient (Fig. 1A), with [H_2O_2] peaking within the first few minutes after growth factor addition and then returning rapidly toward basal levels. This time course is similar to that described for PDGF-induced tyrosine phosphorylation (*8*). Exogenously added H_2O_2 or other oxidant stresses can induce tyrosine phosphorylation in several cell types (*9*). We observed similar effects in VSMCs. Increasing extracellular [H_2O_2] from 0.01 to 10 mM resulted in significant increases in the total amount of tyrosine-phosphorylated proteins (Fig. 1B). To achieve the intracellular [H_2O_2] seen after PDGF stimulation required extracellular [H_2O_2] in the 0.1 to 1.0 mM range (*10*). This range of extracellular [H_2O_2] also appears to induce the tyrosine phosphorylation of the p42 isoform of mitogen-activated protein (MAP) kinase (Fig. 1C).

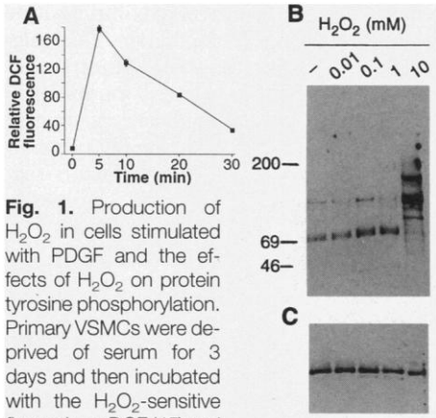

Fig. 1. Production of H_2O_2 in cells stimulated with PDGF and the effects of H_2O_2 on protein tyrosine phosphorylation. Primary VSMCs were deprived of serum for 3 days and then incubated with the H_2O_2-sensitive fluorophore DCF (*17*) and imaged by laser confocal microscopy before and after treatment with PDGF (5 ng/ml). (**A**) Time course of H_2O_2 generation after PDGF stimulation in relative DCF fluorescence units (scale of 0 to 256 units). Values are mean ± SEM obtained from 20 or more random cells. (**B** and **C**) Lysates were prepared from unstimulated VSMCs or VSMCs stimulated for 20 min with increasing concentrations of H_2O_2 (as indicated). Lysates were first immunoprecipitated with an antibody to phosphotyrosine and immunoblots probed with either (B) a phosphotyrosine antibody or (C) an antibody that recognizes the p44 and p42 isoforms of MAP kinase (*18*). Molecular sizes are indicated in (B) in kilodaltons.

We decreased [H_2O_2] in VSMCs by increasing the amount of the peroxide-scavenging enzyme catalase. This enzyme rapidly degrades H_2O_2 to water and molecular oxygen. Infection of VSMCs with an adenovirus that encodes catalase (Ad.Cat) resulted in measurable increases in intracellular catalase activity (Fig. 2A) (*11*). The level of enzymatic activity was a function of the multiplicity of infection (MOI), and no increase was seen when a control adenovirus encoding the *Escherichia coli lacZ* gene (Ad.βgal) was used. Addition of purified catalase to the culture medium resulted in even greater increases in intracellular VSMC catalase activity. Because catalase is a 60-kD protein which in solution forms homotetramers, it seems unlikely that the protein simply diffuses into VSMCs. Indeed, although loading of VSMCs with catalase by addition of the purified enzyme to the medium resulted in a time-dependent increase in VSMC intracellular catalase activity, this was not observed in several other cell lines tested such as human umbilical vein endothelial cells (HUVECs) or HeLa cells (Fig. 2B). Uptake of catalase into VSMCs did not occur at 4°C, suggesting that it is an energy-dependent and perhaps receptor-mediated process (*10*). The increase in intracellular catalase activity was dependent on the concentration of extracellular catalase (Fig. 2C). At the highest extracellular concentration used (3000 U/ml), a 72-hour incubation resulted in a ~50-fold increase in intracellular catalase activity.

To show that the addition of exogenous catalase did not result in its nonspecific binding to the outer surfaces of VSMCs, we loaded cells with catalase and then exposed them to proteinase K. Although proteinase K (1 mg/ml) rapidly inactivated purified catalase in solution, the enzymatic activity of catalase-loaded cells was resistant to the protease (Fig. 2D). We also stimulated VSMCs loaded with catalase with PDGF and assayed for H_2O_2 levels. Catalase-loaded VSMCs had a reduced peak level of DCF fluorescence after the addition of PDGF. The relative peak DCF fluorescence seen after growth factor addition was a function of catalase concentrations (Fig. 2E).

We assessed the effect of increased intracellular catalase activity on PDGF signal transduction. PDGF-AB (5 ng/ml) induced a rapid increase in tyrosine phosphorylation of numerous proteins (Fig. 3A). As catalase activity increased, the PDGF-induced stimulation of tyrosine phosphorylation was correspondingly reduced in a dose-dependent fashion. At the highest amount of intracellular catalase activity, an amount that almost completely blocks the growth factor–induced rise in [H_2O_2], stimulation of tyrosine phosphorylation by PDGF was almost completely inhibited (Fig. 3A).

The addition of catalase even in large amounts (3000 U/ml) for prolonged periods of time (>5 days) produced no visible effects on VSMCs and did not affect viability as assessed by trypan blue exclusion, although catalase-loaded cells grew at approximately half the rate of control cells (*10*). In addition, although catalase-loaded cells had an attenuated response to PDGF, when the NO

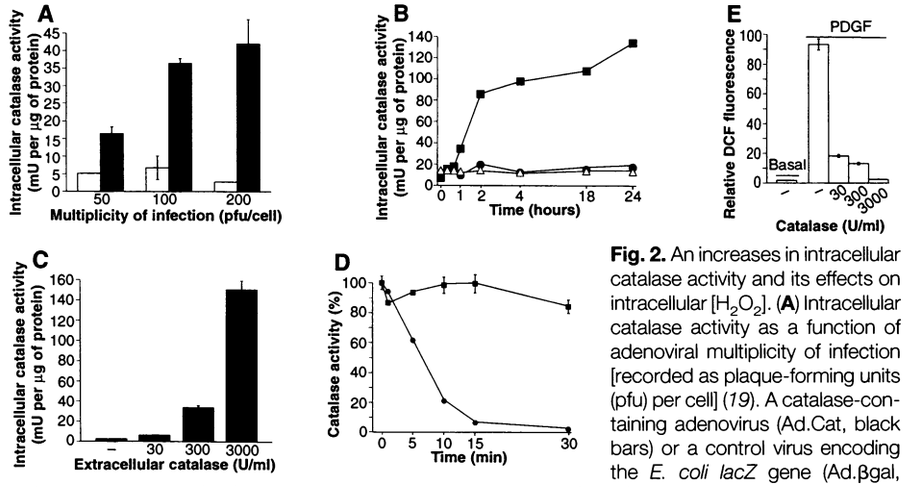

Fig. 2. An increases in intracellular catalase activity and its effects on intracellular [H_2O_2]. (**A**) Intracellular catalase activity as a function of adenoviral multiplicity of infection [recorded as plaque-forming units (pfu) per cell] (*19*). A catalase-containing adenovirus (Ad.Cat, black bars) or a control virus encoding the *E. coli lacZ* gene (Ad.βgal, white bars) was used. (**B**) Time-dependent intracellular catalase activity after exogenous administration of catalase to VSMCs (■), HUVECs (●), and HeLa cells (△) (*20*). (**C**) Intracellular catalase activity as a function of exogenous catalase concentration. (**D**) Effects of proteinase K on catalase activity (*21*). All measurements of catalase activity were obtained from triplicate cultures and are expressed as mean ± SEM. ■, Catalase-loaded cells; ●, purified catalase in solution. (**E**) Representative experiment demonstrating relative DCF fluorescence in unstimulated and PDGF-stimulated cells loaded with catalase. Values were obtained from 20 or more cells and expressed as mean ± SEM.

donor sodium nitroprusside (SNP) was added to the medium there was a rise in the concentration of cyclic guanosine 3′,5′-monophosphate (cGMP) equal to or greater than that of control cells (Fig. 3B). This indicates that the H_2O_2 and NO pathways are separable and that increased intracellular catalase does not have a toxic or global effect on all signal transduction pathways.

We next identified specific proteins whose growth factor–stimulated tyrosine phosphorylation was regulated by endogenous H_2O_2 release. Stimulation of VSMCs with PDGF induced an increase in the amount of tyrosine-phosphorylated p44 and p42 isoforms of MAP kinase. As intracellular catalase activity increased, both basal and PDGF-stimulated tyrosine phosphorylation of MAP kinase were inhibited (Fig. 4A). These results were not due to changes in the steady-state amount of MAP kinase protein in catalase-treated cells (Fig. 4B). Qualitatively similar results were obtained after adenoviral gene transfer. Infection with Ad.Cat (200 MOI) produced intracellular catalase activity that was equivalent to that observed with 72 hours of catalase loading at an intermediate dose (300 U/ml) of extracellular catalase (Fig. 2, A and C). Such infection with either Ad.βgal or Ad.Cat affected cell morphology and in general reduced the responsiveness of VSMCs to growth factors (*10*). Nonetheless, MAP kinase phosphorylation after PDGF addition was inhibited to a greater extent in Ad.Cat-infected compared with similarly infected Ad.βgal cells (Fig. 4C). In accordance with the amount of MAP kinase tyrosine phosphorylation, MAP kinase enzymatic activity [as assessed by phosphorylation of a myelin basic protein (MBP) substrate] varied in relation to catalase activity (Fig. 4D). Consistent with the reduction in MAP kinase phosphorylation and activity, PDGF-induced [^{3}H]thymidine incorporation was reduced in the presence of increased amounts of catalase (Fig. 4E).

Increased amounts of intracellular catalase activity also inhibited the ability of PDGF to stimulate chemotaxis of VSMCs (Fig. 4F). A ~50% reduction in migration was observed at the highest level of catalase activity. The molecular basis of PDGF-induced migration is not fully understood, but it might involve the cytoskeletal-associated protein paxillin, whose tyrosine phosphorylation is stimulated by PDGF in several cell types including VSMCs (*12*). The amount of tyrosine-phosphorylated paxillin in PDGF-stimulated lysates was decreased in cells containing high catalase activity (Fig. 4F, insert).

We tested whether other reactive oxygen intermediate scavengers would have effects similar to those of catalase. When VSMCs were treated with the chemical antioxidant *N*-acetylcysteine (NAC), we noted a concentration-dependent reduction in PDGF-stimulated DCF fluorescence (Fig. 5A). NAC caused a concentration-dependent reduction in PDGF-stimulated tyrosine phosphorylation (Fig. 5B). Similarly, millimolar amounts of NAC resulted in a reduction of PDGF-stimulated MAP kinase phosphorylation and thymidine uptake (*10*).

The mechanism by which H_2O_2 participates in PDGF signal transduction is unclear. Exogenously added H_2O_2 can reversibly inactivate protein tyrosine phosphatases, and enzymatic activity can be subsequently restored by thiol donors (*13*). As such, the growth factor–stimulated rise in [H_2O_2] may serve to transiently inactivate intracellular tyrosine phosphatases, allowing for a temporary alteration in the kinase-phosphatase balance. The magnitude of the rise in intracellular [H_2O_2] may therefore be an important determinant of signal transduction. This is supported by three observations. Exogenous H_2O_2 stimulates MAP kinase phosphorylation over a discrete range (0.1 to 1.0 mM), with 10-fold higher or lower concentrations having less effects (Fig. 1C). Second, cells loaded with catalase at a concentration of 30 or 300 U/ml behaved similarly to control cells in certain assays (MAP kinase activity, [^{3}H]thymidine uptake) but not in others (paxillin tyrosine phosphorylation, chemotaxis). This suggests that differing thresholds of intracellular [H_2O_2] may be required for maximal PDGF stimulation of pathways leading to mitogenesis or migration. Finally, preliminary analysis of other growth factors suggests that stimulation of VSMC by epider-

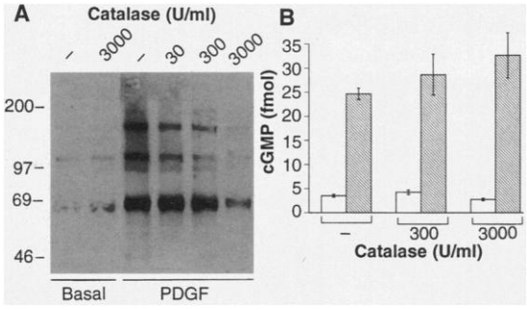

Fig. 3. Effect of increased catalase activity on VSMC signal transduction. (**A**) Immunoblots with antibody to phosphotyrosine of proteins from unstimulated (basal) and PDGF-stimulated cells treated with various amounts of catalase as indicated (*18*). Molecular sizes are shown in kilodaltons. (**B**) Amounts of cGMP 30 min after stimulation with SNP (10 mM) (striped bars) (*22*). White bars, no SNP stimulation. Values are mean ± SEM from triplicate cultures.

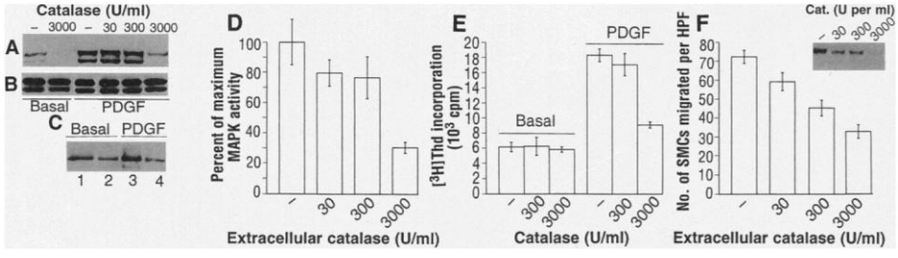

Fig. 4. Effect of inhibition of the H_2O_2 response on PDGF signaling. (**A**) Tyrosine phosphorylation of MAP kinase proteins in unstimulated cells (basal) and cells stimulated with PDGF-AB (5 ng/ml) in the presence or absence of catalase. Lysates were first immunoprecipitated with an antibody to phosphotyrosine, and then the immunoblots were probed with an antibody reactive to p44 and p42 MAP kinase (*18*). (**B**) Total MAP kinase amounts in whole-cell lysates (10 μg of protein per lane). (**C**) Effect of infection with Ad.Cat (lanes 2 and 4) or Ad.βgal (lanes 1 and 3) (200 MOI) on MAP kinase tyrosine phosphorylation. (**D**) Stimulated MAP kinase (MAPK) enzymatic activity as a function of catalase activity (*23*). Results are the mean ± SEM obtained from two separate experiments each performed in triplicate. (**E**) [^{3}H]Thymidine (Thd) incorporation in quadruplicate wells (mean ± SEM) after stimulation of cells with PDGF in the presence or absence of catalase (*24*). (**F**) Effect of intracellular catalase activity on PDGF-stimulated VSMC chemotaxis (*25*). Results are from triplicate experiments and are expressed as the number (mean ± SEM) of migrated VSMC per high-power field (HPF). (**Inset**) Amount of tyrosine-phosphorylated paxillin in PDGF-stimulated lysates as a function of catalase concentrations (*18*).

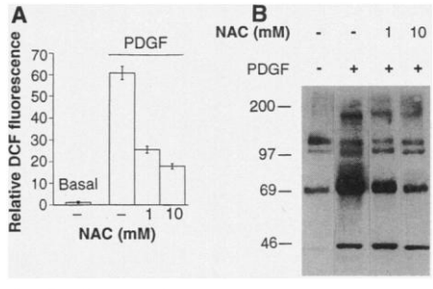

Fig. 5. Effects of the chemical antioxidant *N*-acetylcysteine (NAC) on PDGF signal transduction. (**A**) DCF fluorescence of cells either unstimulated (basal) or stimulated with PDGF as a function of NAC concentration (*26*). Values represent mean ± SEM from 20 or more cells. (**B**) Protein immunoblots of tyrosine-phosphorylated proteins from cells either untreated or treated with PDGF (5 ng/ml) in the presence of the indicated concentration of NAC.

mal growth factor, fibroblast growth factor, or angiotensin II all produce a rise in $[H_2O_2]$ with a correlation existing between the magnitude and duration of an increase in $[H_2O_2]$ and the level of tyrosine phosphorylation (*10*). These latter observations also strengthen the case that in many ways H_2O_2 fulfills the definition of an intracellular second messenger.

VSMCs appear to be unusual in their uptake of extracellular catalase. Certain cells secrete catalase, and the amount of catalase in serum increases in certain disease states (*14*). Thus, growth of VSMCs might be influenced by extracellular catalase in vivo. Recent epidemiological studies suggest a cardioprotective effect of antioxidants (*15*). Given that PDGF-induced VSMC migration and proliferation is thought to precipitate early atherogenic changes (*16*), one mechanism by which dietary antioxidants might protect against cardiovascular events is by a direct effect on H_2O_2-mediated signal transduction in VSMCs.

REFERENCES AND NOTES

1. A. Levine, R. Tenhaken, R. Dixon, C. Lamb, *Cell* **79**, 583 (1994).
2. Z. Chen, H. Silva, D. F. Klessig, *Science* **262**, 1883 (1993).
3. R. Schreck, P. Rieber, P. A. Baeuerle, *EMBO J.* **10**, 2247 (1991); R. Schreck and P. A. Baeuerle, *Trends Cell Biol.* **1**, 39 (1991).
4. D. M. Hockenbery, Z. N. Oltvai, X. Yin, C. L. Millman, S. J. Korsmeyer, *Cell* **75**, 241 (1993); D. J. Kane *et al.*, *Science* **262**, 1274 (1993); G. Haecker and D. L. Vaux, *Trends Biochem. Sci.* **19**, 99 (1994).
5. M. Shibanuma, T. Kuroki, K. Nose, *Oncogene* **5**, 1025 (1990); H. I. Krieger-Brauer and H. Kather, *J. Clin. Invest.* **89**, 1006 (1992); B. Meier *et al.*, *Biochem. J.* **263**, 539 (1989).
6. M. Ohba, M. Shibanuma, T. Kuroki, K. Nose, *J. Cell Biol.* **126**, 1079 (1994).
7. G. N. Rao and B. C. Berk, *Circ. Res.* **70**, 593 (1992).
8. L. T. Williams, *Science* **243**, 1564 (1989).
9. D. Heffetz, I. Bushkin, R. Dror, Y. Zick, *J. Biol. Chem.* **265**, 2896 (1990); F. J. T. Staal *et al.*, *Proc. Natl. Acad. Sci. U.S.A.* **91**, 3619 (1994).
10. M. Sundaresan and T. Finkel, unpublished observations.
11. S. C. Erzurum, P. Lemarchand, M. A. Rosenfeld, J.-H. Yoo, R. G. Crystal, *Nucleic Acids Res.* **21**, 1607 (1993).
12. S. Rankin and E. Rozengart, *J. Biol. Chem.* **269**, 704 (1994); E. A. Clark and J. S. Brugge, *Science* **268**, 233 (1995); H. Abedi, K. E. Dawes, I. Zachary, *J. Biol. Chem.* **270**, 11367 (1995).
13. D. Hecht and Y. Zick, *Biochem. Biophys. Res. Commun.* **188**, 773 (1992).
14. J. A. Leff *et al.*, *Free Radical Biol. Med.* **13**, 143 (1992); P. A. Sandstom and T. M. Buttke, *Proc. Natl. Acad. Sci. U.S.A.* **90**, 4708 (1993).
15. J. M. Gaziano, J. E. Manson, J. E. Buring, C. H. Hennekens, *Ann. N.Y. Acad. Sci.* **669**, 249 (1992); M. J. Stampfer *et al.*, *N. Engl. J. Med.* **328**, 1444 (1993); E. B. Rimm *et al.*, *ibid.*, p. 1450.
16. R. Ross, *Nature* **362**, 801 (1993).
17. Primary VSMCs were obtained from rat thoracic aorta by enzymatic digestion as described [J. H. Campbell and G. R. Campbell, *Vascular Smooth Muscle in Culture* (CRC, Boca Raton, FL, 1987), pp. 15–22] and were stimulated with PDGF-AB (5 ng/ml); DCF fluorescence was measured (*6*). Images were collected with a Leica Laser confocal scanning microscope, model TCD4. Relative DCF fluorescence was recorded on a scale from 0 to 256. In general, basal fluorescence averaged from 0 to 10 units, whereas stimulated fluorescence averaged from 60 to 200 units. Although DCF is oxidized by both H_2O_2 and hydroxyl radicals, the lack of fluorescence in PDGF-stimulated catalase-loaded cells suggests that the fluorescent signal after the addition of growth factor is predominantly derived from H_2O_2 (see Fig. 2E).
18. VSMCs deprived of serum for 3 days were stimulated with the indicated concentration of H_2O_2 or PDGF-AB (5 ng/ml) for 20 min, after which cells were harvested and lysed in RIPA buffer [50 mM tris-Cl (pH 7.5), 150 mM NaCl, 1% NP-40, 0.5% sodium deoxycholate, and 0.1% SDS]. Immunoprecipitation was done from 150 mg of unstimulated or stimulated cell lysate with aphosphotyrosine antibody (4G10, UBI). Immunoprecipitated proteins were divided in equal portions, and tyrosine-phosphorylated proteins from 50 mg of lysate were subjected to SDS–polyacrylamide gel electrophoresis (SDS-PAGE) (4 to 20% gels) and transferred to a nitrocellulose filter. When indicated, filters were probed with either an antibody to phosphotyrosine (RC20), a broadly reactive antibody to MAP kinase (erk1-CT, UBI), or an antibody to paxillin (P13520, Transduction Lab). Amounts of MAP kinase protein were detected from total cell lysates (10 μg per lane) by erk1-CT. Antibody binding was visualized by enhanced chemiluminescence (Tropix).
19. Adenoviral stocks were prepared and titered on 293 cells and used to infect VSMCs as described [R. J. Guzman *et al.*, *Proc. Natl. Acad. Sci. U.S.A.* **91**, 10732 (1994)]. Three days after infection, cells were deprived of serum for 3 days, then triplicate cultures were collected in buffer A [1× phosphate-buffered saline (PBS) (0.0067 M), 10 mM EDTA, 2% Triton X-100, and 0.5% deoxycholic acid] for measurement of enzymatic activity or in RIPA buffer for analysis with antibodies to phosphotyrosine.
20. Confluent VSMCs (1×10^6 cells), HUVECs [American Type Culture Collection (ATCC), Rockville, MD], and HeLa cells (ATCC) that had been deprived of serum were incubated with beef liver catalase (3000 U/ml, Boehringer Mannheim) for various times. After incubation, cells were washed twice in PBS, trypsinized, and lysed in buffer A. Catalase activity was assayed by the rate of decrease in absorbance at 240 nm by the method described by H. Aebi [*Methods Enzymol.* **105**, 121 (1994)].
21. Cells incubated with extracellular catalase (3000 U/ml) were collected, and triplicate cultures were exposed to proteinase K (1 mg/ml) in solution for various times. At the indicated time, cells were quickly sedimented and proteinase K diluted and removed. The cells were subsequently lysed in buffer A. Residual catalase activity was measured as described (*20*).
22. Confluent VSMCs with and without catalase loading were stimulated for 30 min with 10 mM SNP. Cells were subsequently lysed with 6% trichloroacetic acid (TCA). Lysates were neutralized, and equal amounts (2×10^5 cells) were used to determine amounts of cGMP by radioimmunoassay (Amersham) according to the manufacturer's recommendation.
23. Cells were stimulated with PDGF (5 ng/ml) for 20 min, and MAP kinase proteins were partially purified by phenylsepharose chromatography as described [S. Offermanns, *J. Immunol.* **152**, 250 (1994)]. Myelin basic protein (MBP) phosphorylation was used as an index of MAP kinase activity, where 100% activity represents the activity derived from PDGF-stimulated cells in the absence of catalase loading.
24. Confluent VSMCs were maintained in media without serum for 3 days and then, as indicated, stimulated with PDGF-AB (5 ng/ml). After 18 hours, cells in quadruplicate wells were incubated for 3 hours with [^{3}H]thymidine (1 mCi/ml), and TCA-precipitable counts were determined. If VSMCs were stimulated with PDGF in the presence of 0.5% serum, we noted effects on both basal and PDGF-stimulated thymidine incorporation; under serum-free conditions, effects were present only with PDGF stimulation. This was presumably because of the effects of catalase loading on residual growth factors present under 0.5% serum conditions.
25. VSMC migration was measured in response to PDGF stimulation in a mini-Boyden chamber as described [S. Biro *et al.*, *Proc. Natl. Acad. Sci. U.S.A.* **90**, 654 (1993)]. In the absence of PDGF stimulation, there was on average 10 VSMCs per high-power field.
26. A 200-mM stock of NAC was adjusted to pH 7.4 by NaOH, flash frozen, and stored in portions at −80° for up to 1 month. VSMCs were treated with the indicated amount of NAC for 8 hours before stimulation.

27. We acknowledge R. G. Crystal for providing the adenoviral constructs; M. Beaven, Y. F. Zhou, W. S. Kwon, R. Vemuri, and N. Epstein for helpful advice; S. G. Rhee and S. E. Epstein for critical review and helpful comments; and D. Koch for preparation of the manuscript. M.S. was supported by the Howard Hughes Medical Institute as an NIH Research Scholar.

1 June 1995; accepted 21 August 1995

Attenuated *Shigella* as a DNA Delivery Vehicle for DNA-Mediated Immunization

Donata R. Sizemore,* Arthur A. Branstrom, Jerald C. Sadoff†

Direct inoculation of DNA, in the form of purified bacterial plasmids that are unable to replicate in mammalian cells but are able to direct cell synthesis of foreign proteins, is being explored as an approach to vaccine development. Here, a highly attenuated *Shigella* vector invaded mammalian cells and delivered such plasmids into the cytoplasm of cells, and subsequent production of functional foreign protein was measured. Because this *Shigella* vector was designed to deliver DNA to colonic mucosa, the method is a potential basis for oral and other mucosal DNA immunization and gene therapy strategies.

Direct DNA-mediated immunization is an exciting new approach to vaccine development (*1*). We chose to exploit the ability of *Shigellae* to enter epithelial cells and escape the phagocytic vacuole as a method for directing plasmid DNA to the cytoplasm of the host cell for protein synthesis and processing for antigen presentation (*2*). To attenuate the *Shigella* vector, we made a deletion mutation in the *asd* gene encoding aspartate β-semialdehyde dehydrogenase, an essential enzyme that is required to synthesize the bacterial cell wall constituent

Department of Bacterial Diseases, Division of Communicable Diseases and Immunology, Walter Reed Army Institute of Research, Washington, DC 20307–5100, USA.

*To whom correspondence should be addressed. E-mail: dr._donata_sizemore@wrsmtp-ccmail.army.mil

†Present address: Merck Research Laboratories, Post Office Box 4, BL3-3, West Point, PA 19486, USA.